Research Article | Vol. 24, No. 24 | 28 Nov 2016 | OPTICS EXPRESS 28122

Optics EXPRESS

Lock-in detection of photoacoustic feedback signal for focusing through scattering media using wave-front shaping

OMER TZANG AND RAFAEL PIESTUN

Department of Electrical, Computer, and Energy Engineering, University of Colorado, Boulder, Colorado 80309, USA
*omer.tzang@colorado.edu

Abstract: Wave-front shaping techniques enable focusing and imaging through scattering media. Unfortunately, most approaches require invasive feedback inside or behind the sample, or use of spatial correlations (memory effect) limiting the application to specific types of samples. Recent approaches overcome these limitations by taking advantage of acoustic waves via the photoacoustic (PA) effect or via photon tagging. We present a fully analog signal processing lock-in scheme for PA detection to improve focusing through scattering media and to efficiently extract nonlinear photoacoustic signals towards wave-front optimization. Our implementation improves PA feedback performance in terms of SNR, speed, and resolution.

OCIS codes: (110.0113) Imaging through turbid media; (110.5125) Photoacoustics; (110.7348) Wavefront encoding; (180.4315) Nonlinear microscopy.

References and links

1. M. Xu and L. V. Wang, "Photoacoustic imaging in biomedicine," Rev. Sci. Instrum. **77**(4), 041101 (2006).
2. L. V. Wang, *Photoacoustic Imaging and Spectroscopy* (CRC University, 2009).
3. I. M. Vellekoop and A. P. Mosk, "Focusing coherent light through opaque strongly scattering media," Opt. Lett. **32**(16), 2309–2311 (2007).
4. A. P. Mosk, A. Lagendijk, G. Lerosey, and M. Fink, "Controlling waves in space and time for imaging and focusing in complex media," Nat. Photonics **6**(5), 283–292 (2012).
5. I. Freund, "Looking through walls and around corners," Physica A **168**(1), 49–65 (1990).
6. I. M. Vellekoop, A. Lagendijk, and A. P. Mosk, "Exploiting disorder for perfect focusing," Nat. Photonics **4**, 320–322 (2010).
7. O. Katz, E. Small, and Y. Silberberg, "Looking around corners and through thin turbid layers in real time with scattered incoherent light," Nat. Photonics **6**(8), 549–553 (2012).
8. I. M. Vellekoop, "Feedback-based wavefront shaping," Opt. Express **23**(9), 12189–12206 (2015).
9. G. Lerosey, J. de Rosny, A. Tourin, and M. Fink, "Focusing beyond the diffraction limit with far-field time reversal," Science **315**(5815), 1120–1122 (2007).
10. S. Popoff, G. Lerosey, M. Fink, A. C. Boccara, and S. Gigan, "Image transmission through an opaque material," Nat. Commun. **1**(6), 81 (2010).
11. C.-L. Hsieh, Y. Pu, R. Grange, and D. Psaltis, "Digital phase conjugation of second harmonic radiation emitted by nanoparticles in turbid media," Opt. Express **18**(12), 12283–12290 (2010).
12. I. M. Vellekoop, M. Cui, and C. Yang, "Digital optical phase conjugation of fluorescence in turbid tissue," Appl. Phys. Lett. **101**(8), 81108 (2012).
13. X. Tao, O. Azucena, M. Fu, Y. Zuo, D. C. Chen, and J. Kubby, "Adaptive optics microscopy with direct wavefront sensing using fluorescent protein guide stars," Opt. Lett. **36**(17), 3389–3391 (2011).
14. X. Xu, H. Liu, and L. V. Wang, "Time-reversed ultrasonically encoded optical focusing into scattering media," Nat. Photonics **5**(3), 154–157 (2011).
15. B. Judkewitz, Y. M. Wang, R. Horstmeyer, A. Mathy, and C. Yang, "Speckle-scale focusing in the diffusive regime with time-reversal of variance-encoded light (TROVE)," Nat. Photonics **7**(4), 300–305 (2013).
16. D. B. Conkey, A. M. Caravaca-Aguirre, J. D. Dove, H. Ju, T. W. Murray, and R. Piestun, "Super-resolution photoacoustic imaging through a scattering wall," Nat. Commun. **6**, 9 (2015).
17. F. Kong, R. H. Silverman, L. Liu, P. V. Chitnis, K. K. Lee, and Y. C. Chen, "Photoacoustic-guided convergence of light through optically diffusive media," Opt. Lett. **36**(11), 2053–2055 (2011).
18. T. Chaigne, O. Katz, C. Boccara, M. Fink, E. Bossy, and S. Gigan, "Controlling light in scattering media non-invasively using the photoacoustic transmission matrix," Nat. Photonics **8**(1), 58–64 (2013).
19. O. Katz, E. Small, Y. Guan, and Y. Silberberg, "Noninvasive nonlinear imaging through strongly-scattering

#276242 http://dx.doi.org/10.1364/OE.24.028123
Journal © 2016 Received 6 Oct 2016; revised 17 Nov 2016; accepted 18 Nov 2016; published 23 Nov 2016

Optics EXPRESS

turbid layers," Optica **1**(3), 1–10 (2014).
20. J. Tang, R. N. Germain, and M. Cui, "Superpenetration optical microscopy by iterative multiphoton adaptive compensation technique," Proc. Natl. Acad. Sci. U.S.A. **109**(22), 8434–8439 (2012).
21. A. Danielli, K. Maslov, A. Garcia-Uribe, A. M. Winkler, C. Li, L. Wang, Y. Chen, G. W. Dorn 2nd, and L. V. Wang, "Label-free photoacoustic nanoscopy," J. Biomed. Opt. **19**(8), 086006 (2014).
22. J. Yao, L. Wang, C. Li, C. Zhang, and L. V. Wang, "Photoimprint photoacoustic microscopy for three-dimensional label-free subdiffraction imaging," Phys. Rev. Lett. **112**(1), 014302 (2014).
23. A. S. Goy and J. W. Fleischer, "Resolution enhancement in nonlinear photoacoustic imaging," Appl. Phys. Lett. **107**(21), 211102 (2015).
24. P. Lai, L. Wang, J. W. Tay, and L. V. Wang, "Photoacoustically guided wavefront shaping for enhanced optical focusing in scattering media," Nat. Photonics **9**(2), 126–132 (2015).
25. K. Maslov and L. V. Wang, "Photoacoustic imaging of biological tissue with intensity-modulated continuous-wave laser," J. Biomed. Opt. **13**(2), 024006 (2008).
26. Y. Zhao, S. Yang, C. Chen, and D. Xing, "Simultaneous optical absorption and viscoelasticity imaging based on photoacoustic lock-in measurement," Opt. Lett. **39**(9), 2565–2568 (2014).
27. P. Leboulluec, H. Liu, and B. Yuan, "A cost-efficient frequency-domain photoacoustic imaging system," Am. J. Phys. **81**(9), 712 (2013).
28. S.-Y. Lee, Y.-H. Lai, K.-C. Huang, Y.-H. Cheng, T.-F. Tseng, and C.-K. Sun, "In vivo sub-femtoliter resolution photoacoustic microscopy with higher frame rates," Sci. Rep. **5**, 15421 (2015).
29. Y.-H. Lai, S.-Y. Lee, C.-F. Chang, Y.-H. Cheng, and C.-K. Sun, "Nonlinear photoacoustic microscopy via a loss modulation technique: from detection to imaging," Opt. Express **22**(1), 525–536 (2014).
30. D. B. Conkey, A. N. Brown, A. M. Caravaca-Aguirre, and R. Piestun, "Genetic algorithm optimization for focusing through turbid media in noisy environments," Opt. Express **20**(5), 4840–4849 (2012).
31. A. Danielli, K. Maslov, C. P. Favazza, J. Xia, and L. V. Wang, "Nonlinear photoacoustic spectroscopy of hemoglobin," Appl. Phys. Lett. **106**(20), 203701 (2015).
32. A. Prost, F. Poisson, and E. Bossy, "Photoacoustic generation by a gold nanosphere: From linear to nonlinear thermoelastics in the long-pulse illumination regime," Phys. Rev. B – Condens. Matter Mater. Phys. **92**(11), 1–16 (2015).
33. V. P. Zharov, "Ultrasharp nonlinear photothermal and photoacoustic resonances and holes beyond the spectral limit," Nat. Photonics **5**(2), 110–116 (2011).
34. M. Sarimollaoglu, D. A. Nedosekin, Y. A. Menyaev, M. A. Juratli, and V. P. Zharov, "Nonlinear photoacoustic signal amplification from single targets in absorption background," Photoacoustics **2**(1), 1–11 (2014).
35. K. Fujita, M. Kobayashi, S. Kawano, M. Yamanaka, and S. Kawata, "High-resolution confocal microscopy by saturated excitation of fluorescence," Phys. Rev. Lett. **99**(22), 228105 (2007).
36. O. Tzang, A. Pevzner, R. E. Marvel, R. F. Haglund, and O. Cheshnovsky, "Super-resolution in label-free photomodulated reflectivity," Nano Lett. **15**(2), 1362–1367 (2015).
37. O. Tzang and O. Cheshnovsky, "New modes in label-free super resolution based on photo-modulated reflectivity," Opt. Express **23**(16), 20926–20932 (2015).

1. Introduction

Photoacoustic (PA) imaging is a hybrid modality that achieves optical contrast based on the PA effect by which absorption induces a transient thermoelastic expansion and an associated acoustic emission. Since ultrasonic scattering by tissue is 10^3 weaker than optical scattering, PA microscopy is able to produce acoustic resolution images at depths beyond the optical diffusion limit [1]. PA also reveals label-free optical contrast correlated to chemical composition by exciting the sample with different optical wavelengths [2].

Focusing through highly inhomogeneous scattering media has long been considered technically impossible. Recent developments in the field of wave-front shaping have changed this view, demonstrating that scattered light can be controlled and utilized for optical focusing through the media [3,4]. The properties of strongly scattering media [5] can be harnessed for focusing and image transfer across complex samples by iterative wave-front optimization [6–8], time reversal [9], or directly measuring and inverting the transmission matrix [10]. However, all these approaches are not directly applicable once the goal is to focus deep inside scattering media since they require measurements of transmitted light. For focusing noninvasively, feedback based wave-front optimization requires the assistance of beacons or so-called guide-stars in the target location. Guide-stars have successfully been implemented using second-harmonic [11] or fluorescent particles [12,13], but these methods require stationary particles. An alternative, label-free and noninvasive approach, utilizes ultrasound as a guide star. Several recent techniques, including time reversal of ultrasound encoded light [14] and time reversal of variance encoded light [15] show promising preliminary results for

Optics EXPRESS

deep imaging in scattering materials. However their inherent low SNR limits implementation. Direct approaches for focusing light using the PA signal as feedback [16,17] or by measuring the PA transmission matrix [18] are typically richer in SNR but still require significant signal averaging, noise filtering and long acquisition times. Therefore better SNR, faster acquisition and shorter focusing durations are critical for the applicability of these approaches.

In this paper, we present and implement a method for detecting low intensity signals with increased SNR and adapt them specifically for PA detection, wave-front shaping optimization and focusing through scattering media. The method is also designed for efficient detection of nonlinear PA signals. Nonlinear feedback is important for wave-front shaping experiments because it can generate a single diffraction-limited focus even if the speckle field is non-localized (multi-speckle) [19] and therefore highly attractive for high resolution imaging and enhanced penetration depth [20]. Nonlinear PA signals have also been utilized for label-free super-resolution microscopy [21–23]. Most relevant to this work, nonlinear PA has been used for enhancing focusing though scattering media using the Grueneisen relaxation effect [24]. In our work we develop a general method for efficient detection of non-linear signals and direct implementation as feedback for wave-front shaping.

PA imaging systems using an intensity-modulated continuous-wave (CW) laser source have utilized lock-in detection schemes to enhance sensitivity and cost effectiveness [25–27]. However pulsed excitation generates much stronger PA signals while posing detection challenges. For instance, a demodulation scheme using a high repetition rate Ti-Sapphire femtosecond laser, and a lock-in amplifier was applied for nonlinear two-photon absorption PA measurements [28,29]. There, relatively low energy pulses for PA, of a few nJ, at high (80MHz) repetition rate, were used, causing suppression of the transient response of the material. Here we develop a scheme using nanosecond pulses with energy up to 150μJ and measure the significantly higher, transient single-pulse PA signal, along with the advantages of modulation and lock-in detection of any type of nonlinearity. To our knowledge, this detection scheme is unique in terms of the type of PA excitation with high repetition rate pulses, nonlinearity extraction using a lock-in amplifier, and in its use in wave-front shaping feedback.

This paper is organized as follows: In Sec. 2 we introduce the approach and methodology. In Sec. 3 we present the experimental results. Sec. 4 focuses on the detection of nonlinear PA signals, while Sec. 5 discusses advantages and limitations of the approach.

2. Methodology

The detection method (Fig. 1) is based on modulating the PA signal and using a lock-in amplifier. Lock-in amplifiers are known for their ability to detect signals deeply buried in noise by narrowing down the detection bandwidth up to a fraction of Hz around a modulation frequency. The majority of PA measurements are challenged by SNR and therefore a modulation and lock-in scheme could enhance their performance. In particular wave-front shaping optimization in scattering media improves dramatically with high sensitivity [30].

Lock-in detection of PA signals excited by optical pulses requires several signal processing preparation steps in order to extract the modulation envelope. If amplitude modulation is used directly on the PA signal, the generated frequency side-lobes have low energy due to the oscillating positive and negative amplitudes of the PA wave. The sum of those positive and negative amplitudes is much smaller than the actual energy of the modulated signal. In addition the low duty factor of the pulse train decreases the modulation envelope energy. To increase the SNR at the modulated frequency, we implement rectification to flip the acoustic wave to positive values only. Then a Boxcar Integrator transforms the acoustic pulse train to a modulated step response with high energy envelope. We use lock-in detection of the modulated envelope as feedback for the wave-front shaping optimization. Lock-in detection in the modulation reference frequency corresponds to linear

Optics EXPRESS

PA. The fully analog signal processing scheme was developed in order to avoid any deceleration of the acquisition speed.

Figure 1 depicts the analog detection scheme. The PA signal is first amplified by low-noise preamplifiers, and then rectified using an envelope detector (Analog Devices, ADL5511). The full wave rectification flips the negative PA lobes, creating an all positive PA signal with maximized modulation frequency components. The signal is then sampled by a gated boxcar integrator (SRS, SR250). The output contains now a step modulated signal instead of a pulse train. This signal is fed into a lock-in amplifier (Ametek Signal Recovery, 7270) for detection. The step modulated signal contains now the amplitude of the PA signal. Once passed onto the lock-in amplifier, the PA amplitude is extracted and transferred directly to the computer to feed the optimization algorithm.

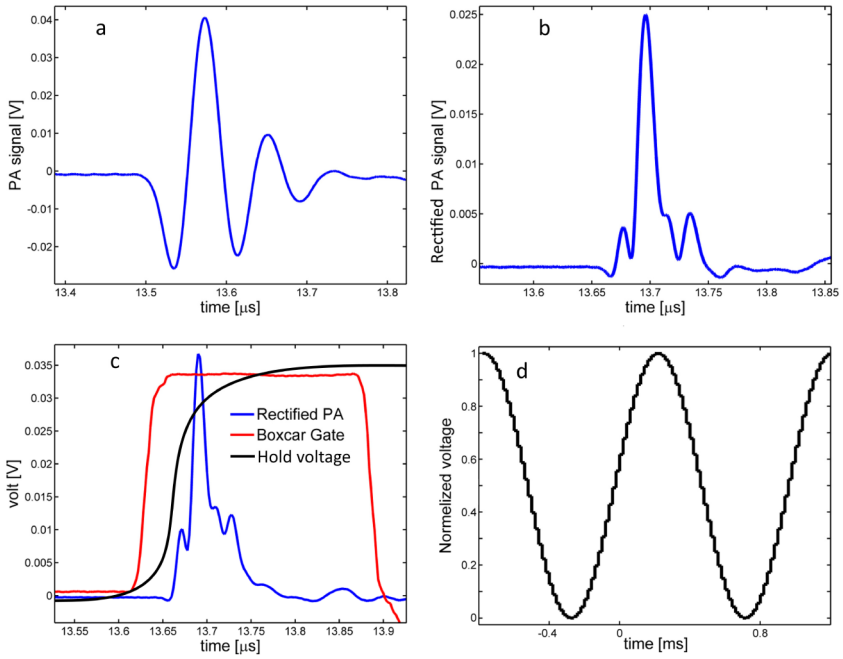

Fig. 1. Analog Signal processing for nonlinear PA. a- Typical PA signal using a 15MHz transducer. b- Rectified PA signal. Note the inversion of the negative lobes in a. c- Single pulse sample and hold circuit, implemented by a boxcar integrator. The gate (Red) shows the specific time window in which the PA signal (blue) is sampled. The integrated voltage (black) is held until the next pulse. d- Schematic, averaged output of the sample and hold circuit. Each pulse has now a discrete value and the modulation sidebands are enhanced with respect to the pulse train.

The photo-modulation is performed using an acousto-optic modulator (AOM) (AA optoelectronic, MTS110) driven by an arbitrary function generator. An important step in our methodology is calculating the AOM driving function. Our external algorithm calculates an optimized driving function to minimize higher harmonics excitation using iterative lookup table. The pure sinusoidal excitation is crucial for nonlinear detection, as discussed later.

Figure 2 depicts the experimental setup for focusing through scattering media using PA feedback. The analog detection scheme and a lock-in amplifier are incorporated and the output is used as optimization feedback.

Optics EXPRESS

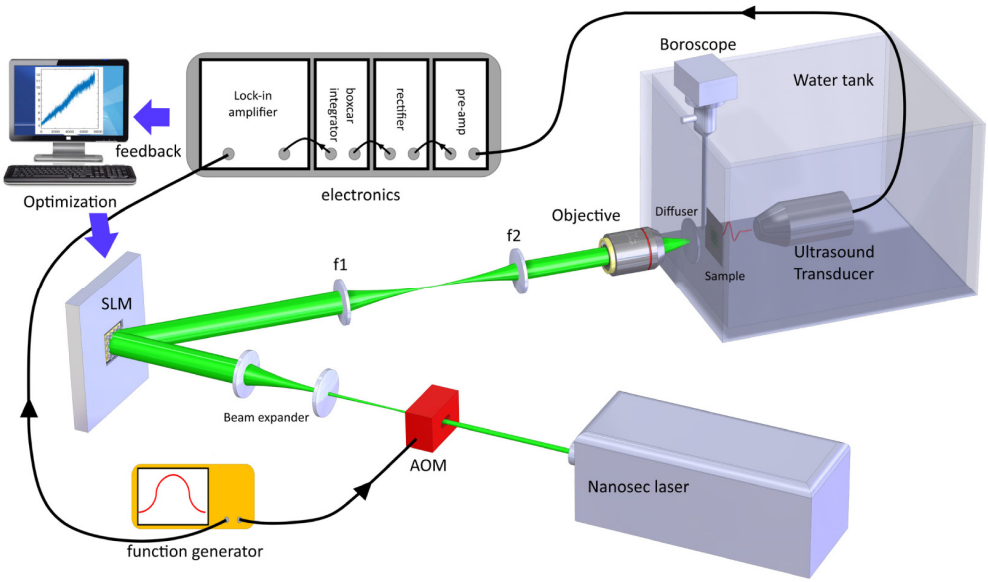

Fig. 2. Experimental setup. A pulsed laser reflected off the SLM and focused on a glass diffuser by an objective. The pulse train is modulated by an AOM at ~1KHz. PA signals from the sample, behind the diffuser, are collected by the acoustic transducer, amplified and analyzed by the analog detection scheme (Fig. 1). A lock in amplifier detects the modulated PA signal and its output is used as a feedback for the SLM optimization. Focusing through the diffuser is optimized using genetic algorithms.

The optical setup includes a laser source (Spectra Physics, Mosaic) with 532nm, ~10ns pulses, energy up to 150μJ and repartition rate of 20 KHz, which is limited only by the maximal frequency of the current Boxcar Integrator. Wave-front shaping is preformed using a liquid crystal spatial light modulator (LC-SLM) (Meadowlark 512x512). Reflected light of the SLM is imaged onto the back aperture of a long working distance microscope objective (Olympus, 0.14 NA) and focuses into a water tank, through a glass diffuser. An absorbing sample approximately 20 mm behind the glass diffuser is mounted onto a three-dimensional translation stage. A 20MHz focusing ultrasound transducer (Olympus, V316, 15MHz, 6db), placed in the water, detects the photoacoustic signal. The optical speckle illumination pattern on the sample is imaged by a Borescope (Gradient Lens Corp, Hawkeye) and recorded during optimization of monitoring and validation.

3. Results

We experimentally demonstrate the ability to localize a scattered light field to a tight speckle field using our detection system. For this demonstration a layer of black electric tape was placed on a glass slide facing the focused transducer. The laser pulse passes through a diffuser, producing an optical intensity pattern on the sample, at the transducer focal plane. For the wave-front optimization we implemented a Genetic Algorithm (GA) as described in [30]. Accordingly, SLM phase patterns are optimized based on the intensity of the detected PA signal (feedback). The process starts with random phase patterns and iteratively converges to an optimized phase mask by natural selections that mimic biological evolution. Upon optimization, the calculated phase mask pre-compensates random scattering events inside the media, the photoacoustic signal is enhanced and a focal point is formed, which is verified via the borescope.

Figure 3(a) and 3(b) depict ‘before’ and ‘after’ speckle patterns using linear optimization. The GA optimization process is depicted in Fig. 3(e). The speckle size at the sample was adjusted by selecting the sample-diffuser distance and slight transducer defocusing such that

Optics EXPRESS

multi-speckles (~10) are located inside the focal area of the transducer. Our calibration measurement shows a focus area, encompassing multiple speckles, of ~300 microns.

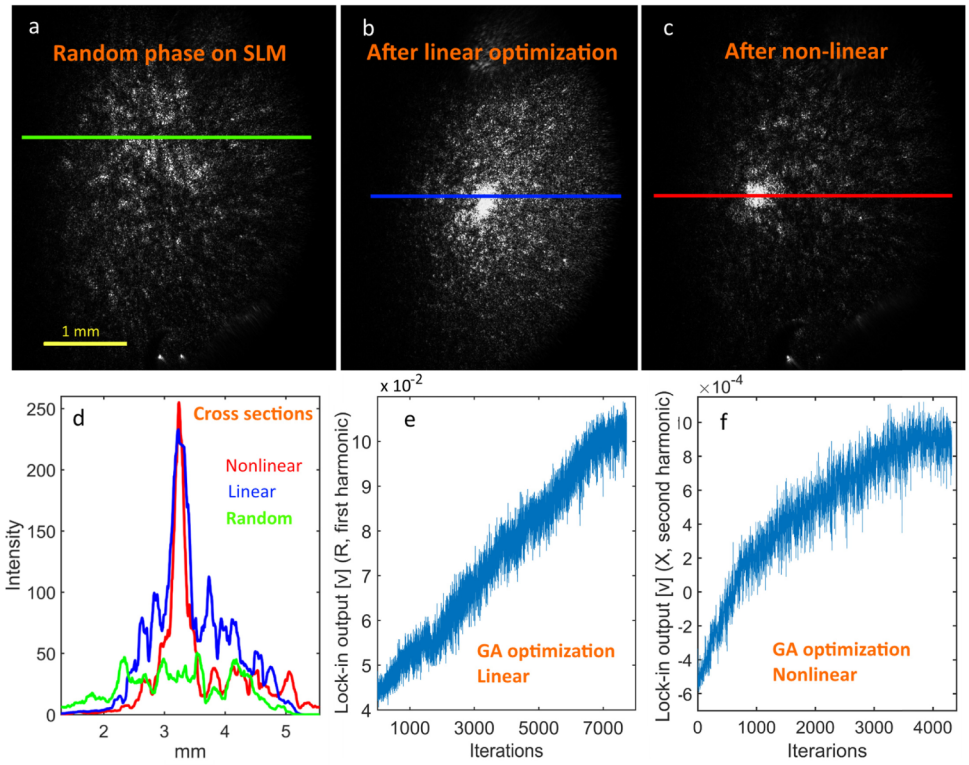

Fig. 3. Results of focusing through scattering media using the lock-in amplifier and analog detection scheme. a- Borescope image of scattered light on a black tape sample. The wave-front phase is random. b-Focusing on black tape using the linear PA feedback from the lock-in amplifier. c- Focusing by non-linear feedback from the lock-in amplifier. The second harmonic of the modulation frequency contains the second order non-linearity of the PA signal. Repetition rate was 19 KHz, and optimized AOM sinusoidal modulation at 1.1 KHz. d- Cross section comparison of a-c. e –GA Optimization progress using linear PA feedback. f- GA optimization using non-linear PA feedback. The plots represent the lock-in output of the whole GA population at every iteration.

The enhancement is proportional to the number of controlled degrees of freedom, N_{SLM}, and inversely proportional to the number of optical modes (speckle grains) whose intensity is enhanced, N_{modes} [18]. In our case the black tape is a uniform absorbing target in which the number of enhanced speckles, as depicted in Fig. 3(b), is $N_{modes} \sim 10$, corresponding to the number of modes within the acoustic focal area of 300 μm. The expected intensity enhancement [18] is $\eta_{expected} = \alpha\left(\frac{N_{SLM}}{N_{modes}}\right) \sim 0.5\left(\frac{256}{10}\right) = 12.8$. Where N_{SLM} are the 16x16 SLM macro pixels. The factor α depends on the type of light modulation that is used and on the intensity distribution over the input channel. Using the Borescope Camera we measured the peak to background ratio, between the intensity at the focus area and the averaged background intensity near the optimized focus [8]. Accordingly, $\eta_{linear} = 9$ and $\eta_{nonlinear} = 16$. The lower experimental enhancement in the linear case was caused by factors such as optical speckle decorrelation during the experiments, noise in the measurements, and the uneven contribution of the SLM pixels to the photoacoustic signal at a given position [18]. The

Optics EXPRESS

nonlinear enhancement is larger than the expected linear PA optimization value due to effective smaller number of modes in the acoustic focal region in the nonlinear optimization.

Therefore, the number of modes in the focal region has decreased by ~1.7, which agrees well with the (acoustic) spot-size reduction of a second order nonlinearity (factor $\sim\sqrt{2}$). Our results of nonlinear feedback in multi-speckle optimization did not reach a single speckle limit [19], which can be attributed to weak nonlinearity of the sample and the SNR limitations. The time for the linear PA optimization was 6 minutes (limited by SLM refresh rate), and for the nonlinear PA optimization approximately one hour (limited by SNR). Application to dynamic biological samples is currently limited because the speckle decorrelation times are typically in the order of milliseconds.

4. Nonlinear PA

The lock-in detection method is also designed for measuring nonlinear PA, motivated by the potential for 3D enhanced resolution. The source of PA nonlinearities [31–34] varies between different samples and excitations and can be classified in the following categories; 1-saturation and damage effects, 2-thermal nonlinearities and 3-phase transformations in the sample or its surroundings. All mechanisms are characterized by a nonlinear relation of the PA amplitude to the laser fluence. The general goal is to measure the nonlinear contributions and use them for focusing tighter and potentially for higher resolution imaging.

In order to extract the nonlinear components of PA we modulated the excitation pulse train $(\text{at}\,\omega_m)$, and demodulate the signal at the corresponding harmonic frequencies $(\omega_m, 2\omega_m, 3\omega_m \ldots)$ in a lock-in amplifier. As shown in optical microscopy examples, if the modulation is purely sinusoidal, the lock-in amplifier's output of the modulated harmonics is proportional to the nonlinear coefficient of the signal [35–37]. Based on this idea, we apply a purely sinusoidal excitation and record the PA signal generated from the absorber.

This task becomes challenging due to the residual nonlinearities remaining in the electronic devices involved in the detection. Such distortions limit the fidelity of the detected PA nonlinearities and are dealt with proper calibration of the system. In order to correct distortions we optimized the AOM excitation with an arbitrary waveform generator. Using a linear PA sample we monitor the modulated PA signal after the analog processing and minimize the higher harmonics, creating a pure sinusoidal modulation, which compensates all the distortions in the system. The developed iterative procedure [36,37] optimizes the arbitrary function generator that drives the AOM to produce a pure PA harmonic modulation generated by a sample in the linear PA regime, namely with low excitation power. At each step a lookup table procedure finds the driving function that produces the expected modulation based on a recorded output of the detection system. Once convergence is reached such that a function is found that modulates the AOM to generate a linear PA output, a final adjustment step is performed by fine tuning the RF amplitude of the AOM device for minimizing the harmonics in the lock-in amplifier further. For the second harmonic feedback, we offset the modulation phase to zero before the optimization, and monitor the X quadrature output, which with zero phase, is equivalent to the amplitude output but unambiguously sensitive to zero crossing.

Later on, when the nonlinear PA effects become prominent, by changing either the sample or laser power, the higher modulation harmonics in the lock-in amplifier are measured and used as feedback for the optimization. Figure 3(c) depicts the speckle patterns after second order nonlinear optimization. The speckle pattern is tighter (x1.57, $\sim\sqrt{2}$) than in the linear case, as depicted in the cross section in Fig. 3(d). The nonlinear GA optimization process is depicted in Fig. 3(f).

Optics EXPRESS

5. Discussion

Next, we discuss and compare our method to that of digital acquisition of PA signals. The overall focusing speed is determined by two parameters: The first one is the acquisition time of a single PA value, and the second is the total duration of the optimization. At each step of the optimization, a phase pattern is projected on the SLM, and once stable, the modulated PA envelope amplitude is measured by the lock-in and its value is read digitally via a USB interface. Therefore, the time per acquisition comprises a constant SLM delay and a signal acquisition time that is defined by the lock-in amplifier time constant. For the black tape sample, the time constant was set to 5ms, faster than the refresh rate of our SLM (~50ms). Therefore, the acquisition was limited by the SLM, and the SNR of the method is sufficient for fast data acquisition. This defined speed includes all parts of the PA acquisition, namely averaging, filtering, and digitizing the final value.

Typical digital acquisition of PA signals include time domain sampling of each pulse, peak to peak measurement, and calculations for extraction of the PA relevant parameters. In order to compare the speed of our analog method to digital signal processing, we performed SNR characterization at different signal levels and measured time durations and SNR. The digital reference was recorded in an oscilloscope, and the calculation considered the state-of-the-art performance of digitizers and computation power. We found that the analog method was advantageous once the detection bandwidth was narrow enough, or, in other words, the lock-in time constant was long enough. At high signal levels, the lock-in method showed improved sensitivity and speed once the bandwidth of detection was <16Hz at a time constant of 10ms. At low signal levels (relating to the SNR of 1.5 in single shot oscilloscope acquisition), we found that the lock-in method showed higher sensitivity than the digital acquisition once the detection bandwidth was <1Hz (time constant >100ms). At shorter time constants, the equivalent time domain digital averaging showed better sensitivity. We suggest two explanations: First, the narrow bandwidth filtering inherently extended the time duration. Secondly, the analog detection scheme, especially the boxcar integrator, introduced additional noise. This noise could be further reduced with improved electronics. The total number of steps of a focusing optimization process in both the digital and analog method is similar.

Experimental parameters such as averaging, detection bandwidth, and filtering can be easily adjusted and optimized for each sample. The repetition rate of our laser was set to <20 KHz, limited by the current Boxcar integrator maximal frequency. With a higher frequency Boxcar, our laser and detection system could be operated at repetition rate of up to 500 KHz, improving by at least one order of magnitude the SNR without additional complication in data acquisition. Potentially, the rep-rate could go up to 1MHz, limited by the overlap of acoustic pulses. An alternative method to rectification and boxcar could be fast digitizing of the signal and synthesizing the modulation amplitude digitally as preparation to lock in detection. This approach would reduce electronic nonlinearities and distortions but require high speed data acquisition that could limit application at high repetition rate lasers.

Nondestructive mechanisms for high SNR nonlinear PA signals are demanded for successful application of the nonlinear lock-in method. The black tape sample used in the demonstration possess an intense PA signal but its saturation nonlinearity appears at high laser intensities which are close to the optical damage threshold of the sample. This proximity to damage processes of the PA nonlinearity limits the applicability of the nonlinear feedback. Hence, PA contrast agents with high nonlinearity at low excitation energy are demanded. For instance, nanoparticles with reproducible nonlinearity are attractive as nonlinear PA contrast agents for wave-front optimization feedback due to their low energy nonlinearity. The absorption wavelength can be tuned by the particle size while PA nonlinearities, associated with bubble formation, could be exploited for wave-front shaping feedback.

Optics EXPRESS

6. Conclusions

In conclusion, we presented a method for PA detection and implementation in wave-front shaping with higher sensitivity compared to conventional PA detection. We used standard experimental lab equipment (arbitrary function generator, lock in amplifier and boxcar integrator) and found the method to work well in low signal and high noise environment. The SNR of the method is expected to improve with increased repetition rate.

The flexibility of directly using linear and/or n^{th} order nonlinearity as the focusing feedback is an important advantage of the method. Moreover, dual/multi harmonic detection of the linear and non-linear components could be combined in a dynamic adaptive feedback. Compared to nonlinear PA detection schemes such as dual pulse extraction of the Grueneisen parameter [24], and extraction of non-linear coefficients by modulated pulse series [21], our analog method can deal better with high repetition rate lasers, noisier signals, and high data acquisition rate, and holds promise for effective detection of PA nonlinearities.

Funding

National Science Foundation (NSF) (1611513).

Acknowledgments

We thank Antonio Miguel Caravaca Aguirre, Jian Wei Tay and Ori Cheshnovsky for useful discussions.